Lithium iodide effect on the electrochemical behavior of agarose based polymer electrolyte for dye-sensitized solar

ARTICLE *in* ELECTROCHIMICA ACTA · AUGUST 2011

Impact Factor: 4.5 · DOI: 10.1016/j.electacta.2011.06.032

3 AUTHORS, INCLUDING:

Weijia Wang
Central South University
2 PUBLICATIONS **20** CITATIONS

SEE PROFILE

Ying Yang
Central South University
35 PUBLICATIONS **524** CITATIONS

SEE PROFILE

Effect of Lithium Iodide Addition on Poly(ethylene oxide)−Poly(vinylidene fluoride) Polymer-Blend Electrolyte for Dye-Sensitized Nanocrystalline Solar Cell

Ying Yang,[†] Jing Zhang,[†] Conghua Zhou,[†] Sujuan Wu,[†] Sheng Xu,[†] Wei Liu,[†] Hongwei Han,[†] Bolei Chen,[†] and Xing-zhong Zhao*[,†,‡]

Department of Physics and Key Laboratory of Acoustic and Photonic Materials and Devices of Ministry of Education, Wuhan University, Wuhan 430072, People's Republic of China

Received: November 26, 2007; Revised Manuscript Received: March 14, 2008; In Final Form: March 20, 2008

The effect of lithium iodide concentration on the conduction behavior of poly(ethylene oxide)−poly(vinylidene fluoride) (PEO−PVDF) polymer-blend electrolyte and the corresponding performance of the dye-sensitized solar cell (DSSC) were studied. The conduction behavior of these electrolytes was investigated with varying LiI concentration (10−60 wt % in polymer blend) by impedance spectroscopy. A "polymer-in-salt" like conduction behavior has been observed in the high salt concentration region. The transition from "salt-in-polymer" to "polymer-in-salt" conduction behavior happened at the salt content of 23.4 wt %, which is much lower than 50 wt % as generally reported. The electrolyte shows the highest ionic conductivity ($\sim 10^{-3}$ S cm^{-1}) at the salt concentration above 23.4 wt %. From the evaluation of salt effect on the performances of corresponding DSSC, we find that increasing LiI concentration leads to increased short-circuit photocurrent density (J_{sc}) caused by enhanced I_3^- diffusion up to an LiI content of 28.9 wt %. Above this limitation, the J_{sc} decreases as a result of increased charge recombination caused by the further increased I_3^- concentration. The open-circuit voltage (V_{oc}) increases gradually with LiI concentration owing to the enhanced I^- content in DSSC. The optimized conversion efficiency is obtained at a salt content of 28.9 wt % in the "polymer-in-salt" region, with high ionic conductivity (1.06×10^{-3} S cm^{-1}). Based on these facts, we suggest that the changes of conduction behavior and the changes of I_3^- and I^- concentrations in the electrolytes contribute to the final performance variation of the corresponding DSSC with varying LiI concentration.

Introduction

In the search for more efficient, clean, and low cost energy storage methods, dye-sensitized solar cell (DSSC) has been attracting much attention, which was first reported by Grätzel in 1991.[1] A photo-to-current conversion efficiency of more than 11% has been achieved in a liquid-electrolyte-based DSSC.[2] To avoid the leakage and evaporation of organic solvent, many efforts have been made to replace the liquid electrolyte by solid-state medium.[3–7] Among these studies, the development of flexible gel or solid polymer electrolyte with high ionic conductivity is of fundamental importance. So far, several methods of modifying polyether electrolyte such as copolymerization[8,9] and coblending[10,11] have been studied to enhance ionic conductivity and photo-to-current conversion efficiency of DSSC.

"Polymer-in-salt" conduction behavior, a high ionic conductive behavior observed in high salt concentration (exceeding 50 wt %) electrolyte, was first proposed by Angell et al.[12] In this electrolyte, the ionic conductivity increases with increasing salt concentration beyond a limitation and the high ionic conductivity is only observed in the salt-rich composition regime (e.g., N:Li ratios exceeding 4:1 for PAN−$LiCF_3SO_3$ complexes[13,14]). It is assumed that, the "polymer-in-salt" conduction behavior is related to a high degree of ionic aggregation. When the aggregates are sufficiently large and numerous, they effectively connect and form a continuous pathway to support ionic movement. Such conduction behaviors are studied most in polyacrylonitrile (PAN) and acrylonitrile−butadiene copolymer electrolytes for lithium battery.[15–17] The reason these systems are promising in lithium battery is that the ionic conductivities depend not on segmental motion of the polymer but the ionic mobility. That is, these electrolytes show decoupled ion transport behavior in a wide range of temperature and provides higher Li^+ transport number.[18] Unfortunately, in spite of high ionic conductivity, they are not suitable for DSSC. A good performance of most DSSC is dependent on an efficient transport of iodide and triiodide (I^-/I_3^-) rather than a high Li^+ transport in the electrolyte. The intercalation or adsorption of Li^+ to the surface of TiO_2 results in a dramatic drop in the open-circuit voltage of DSSC.[19]

In contrast to this, "salt-in-polymer" conduction behavior, of which the conductivity first increases with salt content until reaching a maximum and then decreases at high salt concentrations, is formed by dissolving salts in PEO or other ion-coordinating polymers within limited salt content. This electrolyte shows low cationic transport numbers (close to 0.1 ∼ 0.3), and the ionic conductivity of it is dominated by anionic motion because of strong cation−polymer interaction in chains.[20,21] As a result of this, it shows inferior performance for lithium battery compared with PAN-based electrolyte. But for DSSC, efficient anionic motion (I^-) is what it needed, as mentioned above. Stergiopoulos et al.[22] and Kim et al.[23] reported all-solid-state dye-sensitized solar cells using a poly(ethylene oxide) (PEO) polymer electrolyte modified by inorganic oxide nanoparticles and achieved high energy conversion efficiencies

* To whom correspondence should be addressed. E-mail: xzzhao@whu.edu.cn. Fax: +86-27-87642569. Phone: 86-27-87642989-2784.
† Department of Physics.
‡ Key Laboratory of Acoustic and Photonic Materials and Devices of Ministry of Education.

10.1021/jp801156h CCC: $40.75
Published on Web 05/06/2008

of about 4.2% (under 65.6 mW.cm^{-2}) and 4.5% (under 1 sun illumination (100 mW.cm^{-2})). However, the conductivity maximum of polyether based electrolyte is generally found at intermediate compositions (e.g., ether oxygen to cation ratios of 15:1 for systems based on PEO or PPO[24,25]). Such a low salt concentration (The "salt" means LiI in DSSC) cannot provide a sufficient transport of iodide and triiodide for the cell to reach high performance. Furthermore, a high salt concentration (increasing the salt concentration) leads to a drop in ionic conductivity in this electrolyte (i.e., "salt-in-polymer" conduction behavior). So, it is necessary to study the conduction behavior of this polyether electrolyte in the higher salt concentration region, expecting to get better cell performances and ionic conductivity. Meanwhile, since an undesirable charge recombination is enhanced by the increasing content of I_3^- formed via the interaction of iodine (I_2) and iodide (I^-) as the LiI concentration increases, a study about salt effect on the performance of DSSC with this electrolyte is also required.

Polymer blending technique is extensively used in preparing polymer electrolyte to get better electrical, thermal, and mechanical properties, for its ease of preparation and easy control of physical properties within the compositional regime. Jacob et al.[26] reported a solid polymer electrolyte by introducing poly(vinylidene fluoride) (PVDF) into a PEO−$LiClO_4$ system, which increased the ionic conductivity by 2 orders of magnitude. PVDF, in the presence of fluorine, which has the smallest ionic radius and the largest electronegativity, is expected to improve the ionic transport and reduce the recombination rate at semiconductor/polymer electrolyte interface in DSSC. These merits prompted us to investigate the compatibility of PVDF in the presence of PEO as a host for polymer electrolyte in DSSC. Since 2004, a series of polymer electrolytes based on poly(ethylene oxide)−poly(vinylidene fluoride) (PEO−PVDF) polymer blend have been studied in our group.[27,28] The compatibility and photoelectrochemical behavior of polymer-blend electrolyte by introducing PVDF and TiO_2 into PEO have been studied.[27] This solid electrolyte based on PEO−PVDF showed good miscibility and improved ionic conductivity and achieved a high photo-to-current conversion efficiency of 4.8% under the illumination of 65.2 mW cm^{-2} (AM 1.5), compared to that of pure PEO polymer electrolyte.

As mentioned above, the polyether-based polymer electrolyte possesses several merits for DSSC. This electrolyte has always been considered to be the kind of "salt-in-polymer" one, and there are rarely reports on the "polymer-in-salt" conduction characteristic of this system. Meng et al. reported a "polymer-in-salt" conduction behavior in a solid electrolyte only composed of small molecules (HPN)[29] and employed this electrolyte in DSSC, reaching a light-to-current conversion efficiency as high as 5.4%.[30] In this paper, we attempt to study the conduction behavior of a PEO−PVDF polymer blend electrolyte in the high salt concentration region and try to find a balanced point with relatively sufficient I^-/I_3^- concentration, high ionic conductivity, and optimized cell performance in DSSC. Therefore, the PEO−PVDF polymer-blend electrolyte with wide lithium iodide concentration (10−60 wt % in polymer blend) and the photoelectric performances of the corresponding DSSC as a function of LiI content are studied. In order to understand the nature of conduction in salt-rich electrolytes, the thermal (DSC), FTIR, and SEM characteristics of the PEO−PVDF polymer-blend electrolytes were investigated. To get better understanding of the salt effects on the corresponding DSSC performances, the UV−vis spectra study was employed.

Experimental Section

Reagents. Poly(ethylene oxide) (PEO, $M_w = 2 \times 10^6$g/mol, Aldrich), Poly(vinylidene fluoride) (PVDF, $M_w = 1 \times 10^5$ g/mol, Shanghai, China), lithium iodide (LiI, 99%, Acros), iodine (I_2, 99.8%, Tianjin, China), propylene carbonate (PC, 99.9%, anhydrous, SCRC, China), 1,2-dimethoxyethane (DME, 99.0%, SCRC, China), TiO_2 (P25, 20−30 nm, Degussa AG, Germany) and fused SiO_2 (aerosil 200, 12−15 nm, Degussa AG, Germany) were used in this study. All chemicals were stored in vacuum desiccators before use and used without further purification.

Preparation of PEO−PVDF Polymer-Blend Electrolytes. In our experiment, 0.2 g of the polymer blend with PEO/PVDF = 2:3 wt % was dissolved in 10 g of DME/PC (3:7, v/v) cosolvent under continuous stirring at 80 °C in silicone bath. After about 4 h, fused SiO_2 nanoparticles (0.0291 g) were slowly introduced. This mixed solution was stirred at 80 °C for another 2 h. Then the solid LiI and I_2 with various LiI concentrations (10−60 wt %) and LiI/I_2 = 10:1 (molar ratio) were added at ambient environment. (Here, the "LiI concentration" means LiI/(PEO + PVDF + LiI).) The polymer solution was stirred continuously for almost 4 days in the hermetic brown flask until a homogeneous viscous liquid was formed. The polymer-blend electrolyte membranes were prepared by casting the polymer-blend solutions on glass and placing it in an oven at 80 °C for 12 h to evaporate the solvents.

In order to compare with the PEO−PVDF polymer-blend electrolytes, two series of electrolytes based on the homopolymers of PEO (0.08 g) and PVDF (0.12 g) with varying LiI content (10−90 wt %) were prepared in the same way the PEO−PVDF polymer-blend electrolytes were fabricated. The salt concentration of 10−90 wt % refers to LiI/(PEO + LiI) and LiI/(PVDF + LiI) in the PEO and PVDF based electrolytes, respectively.

Fabrication of Dye-sensitized TiO_2 Photoanode. Nanocrystalline TiO_2 film was fabricated by a doctor-blading technique. The TiO_2 (P25) paste was deposited on a conducting glass substrate (F-doped SnO_2, 15 Ω/square), followed by sintering at 450 °C for 30 min. The thickness of the film was 10 μm. The TiO_2 film was preheated at 120 °C for 30 min before it was immersed into the solution of the dye N3 ($Ru(dcbpy)_2(NCS)_2$, Solaronix) with a concentration of 0.5 mM in dry ethanol overnight.

Assembly of the Dye-Sensitized Solar Cell. The electrolyte solution was dripped onto the dyed TiO_2 film. Then, the solvent was removed under 80 °C in oven. Finally, a sandwich-type DSSC configuration was fabricated by holding the platinum plate counter electrode together with the TiO_2/electrolyte with two clips. The measurements were performed in air. It should be noted that no 4-*tert*-butylpyridine was added into the electrolyte.

Measurements. ***DSC and FTIR Studies.*** Netzsch DSC 200PC (Germany) was used to measure the glass transition temperature (T_g) and melting temperature (T_m) of the polymer electrolytes at a heating rate of 5 °C/min from −100 to 200 °C under N_2 environment. The PEO−PVDF polymer-blend electrolyte films were placed in hermetically closed aluminum vessels for this measurement. FT-IR measurements of the thin polymer electrolyte membranes were performed on a NEXUS670 (Nicolet) FT-IR spectrometer from 4000 to 400 cm^{-1} using the transmission mode.

Impedance Spectroscopy. The ionic conductivity of the polymer-blend electrolyte films were determined with an alternating current (AC) impedance technique on an AC

impedance analyzer (Agilent 4294A, USA) from 40 Hz to 1 MHz between 20 and 80 °C (293 and 353K) with signal amplitude of 10 mV. The polymer electrolyte was melted before a "platinum/electrolyte/platinum" type cell was assembled. The ionic conductivity σ of the membrane is calculated by the following equation,

$$\sigma = L/AR_b \quad (1)$$

Here L is the thickness of the polymer electrolyte membrane and A is the area of the electrode. The resistance (R_b) was taken at the intercept of the Nyquist plot with the real axis. The temperature dependent conductivity of the polymer membrane was measured using a benchtop type temperature and humidity chamber (Espec, Japan).

Transfer Number Measurement. Li^+ transference numbers were obtained using the DC potentiostatic polarization method combined with AC impedance technique proposed by Bruce and Vincent.[31] The DC and AC data were recorded by Agilent 4200 and EG&G model BES impedance analyzer. A symmetrical Li| (Polymer)−LiI |Li cell was assembled in a glovebox in a hermetic Teflon model. The frequency range of the complex impedance plots was $0.1-10^5$ Hz, and the applied DC potential was 500 mV. The Li^+ transference[32,33] numbers of the experimental cell was evaluated by the equation as follows:

$$t_+ = I_\infty(V - I_oR_{eo}) / I_o(V - I_\infty R_{eo}) \quad (2)$$

or

$$t_+ = R_{bo} / (V/I_\infty - R_{e\infty}) \quad (3)$$

where R_{eo} and $R_{e\infty}$ are the electrode resistance before and after DC polarization, respectively, R_{bo} is the bulk resistance, I_o and I_∞ are the initial and the steady-state current, respectively, and V is the voltage of the polarization experiment. The t_+ values estimated by eq 2 are of low differences compared to that calculated by eq 3 normally.[34]

SEM Studies. The Surface morphologies of the polymer-blend electrolyte films with different salt concentration were observed by scanning electron microscope (Sirion FEG, USA).

Photoenergy Conversion Characterization. Photon-to-current conversion efficiencies of the DSSC were evaluated by using a solar light simulator (Oriel, 91192) as the light source and a computer-controlled Keithley 2400 digital source meter unit (USA) as the current−voltage curve recorder. The intensity of the incident light was calibrated by a Si-1787 photodiode (spectral response range = 320−730 nm). The active DSSC area was controlled at 0.25 cm^2 by a mask. All of the measurements mentioned above were taken under ambient conditions.

UV−vis Spectra Studies. I_3^- and I^- absorption was performed in a U-shaped quartz tube with a quartz frit to support the sample by a UV−vis−NIR Spectrophotometer (CARY 5000, Varian). The polymer-blend electrolytes were dissolved in PC/DME cosolvent for this measurement.

Result and Discussion

DSC and FTIR Characteristics of Electrolytes Containing High Lithium Iodide Concentrations and PEO−PVDF Matrixes. Differential scanning calorimetry (DSC) thermograms of pure PEO, PVDF, PEO−PVDF blend, PEO−PVDF-SiO_2 composite, and the polymer-blend electrolytes with lithium iodide comprising from 13.2 to 54.9 wt % are shown in Figure 1 in the range between −100 and 200 °C. From the DSC thermograms, the glass-transition temperature (T_g), the melting temperatures of PEO (T_{m1}), PEO-salt complex (T_{m2}) and PVDF (T_{m3}) were determined. Here, T_m was obtained as the peak of the melting endotherm and T_g as the inflection point.

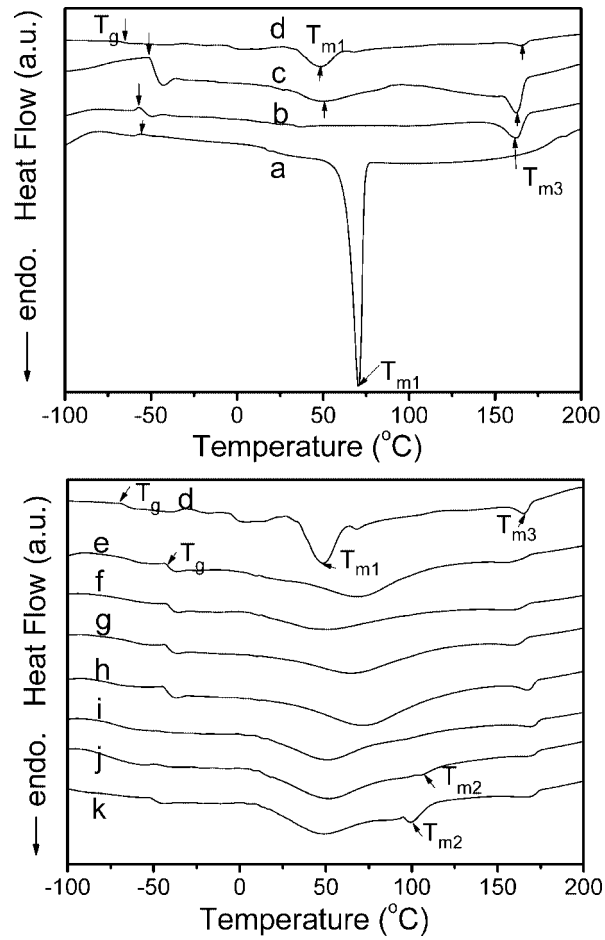

Figure 1. DSC thermograms for (a) pure PEO, (b) pure PVDF, (c) pure PEO−PVDF blend, and DSC thermograms for poly(ethylene oxide)−poly(vinylidene fluoride) polymer-blend electrolytes with various LiI concentrations (wt %): (d) 0 (PEO−PVDF−SiO_2 composite without salt), (e) 13.2, (f) 14.8, (g) 16.9, (h) 23.4, (i) 28.9, (j) 37.9, and (k) 54.9%.

As seen in Figure 1, pure PEO (Figure 1a) shows an acute and intense melting endotherm at 70.6 °C, exhibiting a large degree of crystallinity. A broadened melting endotherm and a lower melting temperature are observed when blending PVDF into PEO (Figure 1c), indicating an evident reduction in crystallinity of PEO. Both the PEO−PVDF (Figure 1c) and the PEO−PVDF−SiO_2 blends (Figure 1d) exhibit a single glass transition (T_g) at −51.3 and −69.7 °C, respectively, which suggests that all the compositions are miscible with the homogeneous phase in the polymer-blend electrolytes, as found previously.[27] The melting points around 48.4 and 168 °C of the pure PEO−PVDF−SiO_2 polymer blend (Figure 1d) are attributed to PEO and PVDF, respectively. Upon addition of salt, all PEO−PVDF polymer-blend electrolytes (Figure 1e−k) exhibit a broadened melting endotherm of PEO around 50−70 °C, indicating a certain reduction in crystallinity of PEO compared to that of pure PEO−PVDF−SiO_2 polymer blend. Furthermore, as the salt concentration exceed 28.9 wt % (Figure 1j,k), the effect of melting at about 100 °C results from the intermediate crystalline complexes formed between the salt and PEO,[35] and it is probably related to the melting of the crystalline complexes formed between the salt ionic agglomerates and PEO.

Changes in T_g as a function of the LiI concentration are depicted in Figure 2 for PEO−PVDF polymer-blend electro-

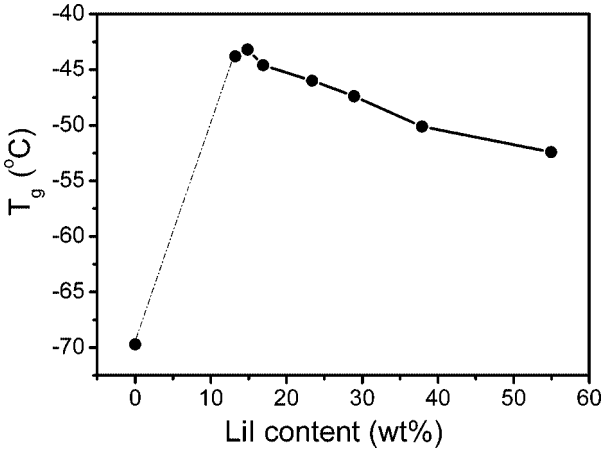

Figure 2. Glass transition temperature, T_g, of poly(ethylene oxide)−poly(vinylidene fluoride) polymer-blend electrolytes as a function of the the salt concentration.

TABLE 1: Absorption Bands (ν_{COC}, ν_{CH}, ν_{CF}, ν_{OH}) in FTIR Spectra of Poly(ethylene oxide)−Poly(vinylidene fluoride) Polymer-Blend Electrolytes with Various Salt Concentrations

LiI content[a] (wt %)	EO:Li[b] (molar ratio)	ν_{COC} (cm^{-1})	ν_{CH} (cm^{-1})	ν_{CF} (cm^{-1})	ν_{OH} (cm^{-1})
0		1112	2873	1407	3483
13.2	8	1104	**2876,**[c] 2911	1408	3448
14.8	7	1101	**2877,** 2913	1407	3448
16.9	6	1097	2878, **2918**	1407	3448
23.4	4	1097	2879, **2920**	1407	3424
28.9	3	1096	2880, **2921**	1407	3427
37.9	2	1093	2881, **2923**	1407	3421
54.9	1	1069	2929	1406	3337

[a] LiI content means LiI/(PEO+PVDF+LiI) in polymer-blend electrolytes. [b] EO:Li refers to the molar ratio of EO units in PEO with LiI in PEO−PVDF polymer electrolytes. [c] Bold font indicates the comparative intense band.

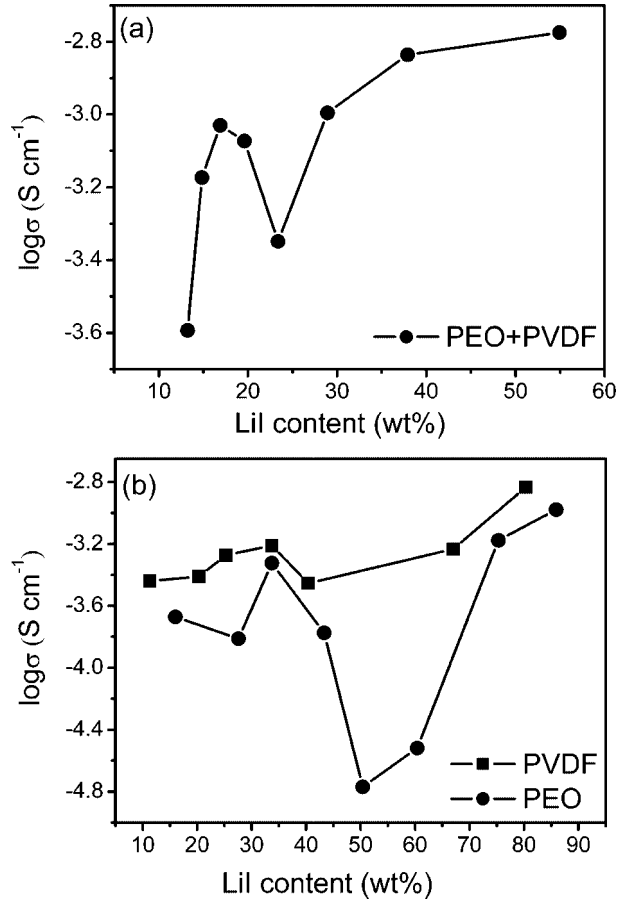

Figure 3. Conductivity isotherms determined at 30 °C for (a) poly(ethylene oxide)−poly(vinylidene fluoride) polymer-blend electrolytes and (b) poly(ethylene oxide) and poly(vinylidene fluoride) polymer electrolytes with varying salt concentration.

lytes. As is seen, the T_g value increases with adding salts because of the increased ion−polymer interactions. These values of T_g at low LiI concentration have not been measured and the dotted line is speculation based on the measured behavior in the PPO:$LiClO_4$ system.[36] At high salt concentrations, the T_g value levels off, which has been commonly observed beyond the solubility limit of the salt in a polymer matrix.[37,38] Although the T_g begins to decrease, the values of T_g are still higher than that of the pure polymer blend.

The interaction of salt with the polymer can be observed by the changes in the vibration frequencies of the polymer matrix. It is known that lithium salts form complexes with C−O−C and O−H groups, which results in a decrease in the frequency of the stretching vibrations of these groups in the FTIR spectra.[39,40] Table 1 lists the absorption bands (ν_{COC}, ν_{CH}, ν_{CF}, ν_{OH}) in FTIR spectra of PEO−PVDF polymer-blend electrolytes with various salt concentrations. As the salt concentration increases, the position of C−O−C stretching vibration maximum shifts from 1112 to 1069 cm^{-1}, accompanying with a split and an upshift of the C−H stretching modes of the $-CH_2$ group in PEO. This indicates that the strength of C−O−C bonding of the polymer matrix is reduced while that of C−H is reinforced, due to the formation of the $Li^+\cdots OC$ associates in the electrolytes. The splitting of the C−H stretching modes leads to a new band appearing around 2910 cm^{-1}, which may be induced by the C−O−C group engaged in complexes with positive salt ions, in addition to the band of noninfluenced free C−H group around 2873 cm^{-1}. It can be seen that the position of C−F stretching mode in PVDF is unchanged as the salt concentration increases. This result illustrates that the matrix polymer PVDF have no effect on the lithium ion or ion cluster of the salt. A lower shift of the O−H stretching vibration is observed from 3482 to 3363 cm^{-1} when LiI concentration increases from 0 to 54.9 wt %. (The value 0 means that no LiI is added into electrolyte.) For poly(ethylene oxide) of M_w = 2 000 000 g/mol, the concentration of the terminal OH groups is very small and could not be observed in the FTIR spectra. This lower shift of the −OH vibration band as the salt concentration increases may be mainly originating from the fused SiO_2 nanoparticles within the polymer blend electrolyte, because there are abundant surface Si−OH groups existing on the SiO_2 nanoparticles.[41,42] It should be noted that, even after heating over 12 h at 80 °C, there is still a small amount of the PC solvent left in the polymer electrolyte films, which can be proved by the small peak of C═O vibration band around 1790 cm^{-1}.

The results presented show a strong interaction between the salt with the polymer matrix. These interactions are observed in the form of a crystal complex between the salt and the polymer in DSC traces and a downshift about 40−50 cm^{-1} of C−O−C vibration bands in the IR spectra. The magnitude of these effects depends on the salt concentration, which is probably related to the solubility of the salt in polymer blend and its complexes with the polymer matrix.

Ionic Conductivity of PEO−PVDF Polymer-Blend Electrolytes Comprising Various Salt Concentrations. Figure 3a illustrates the dependence of the conductivity on LiI concentra-

tion in the PEO−PVDF polymer-blend electrolyte at 30 °C. The conductivity of PEO−PVDF polymer blend without salt is about 2.10×10^{-5} S cm^{-1}. With the addition of salt, a drastic increase in conductivity occurs until a maximum value of 9.26×10^{-4} S cm^{-1} is reached at the salt concentration of 16.9 wt % (EO:Li = 6), after which a further increase in concentration causes a drop in conductivity until 23.4 wt %, followed by another increase. We have discreetly studied this behavior and found that it is well reproducible. The best conductivity in the salt concentration studied is 1.68×10^{-3} S cm^{-1} at 54.9 wt %, equal to EO:Li = 1. Clearly, the above salt concentration dependence of the conductivity is consistent with the "salt-in-polymer" like conduction behavior in the low salt concentration (≤23.4 wt %) and similar to the "polymer-in-salt" like conduction behavior in the high salt concentration range (>23.4 wt %) though there is still little solvent (PC) in our samples. A similar "polymer-in-salt" like conduction behavior was also observed in the PAN−PC−LiTFSI system with increasing salt concentration with solvent (PC) existing in the polymer electrolyte by Wang et al.[43] By controlling the same content of solvent remaining in all polymer electrolyte films during the experimental processes, we considered that the "polymer-in-salt" like conduction behavior of the polymer blend electrolyte studied is dominated by the effect of salt.

An increase in conductivity with increasing of salt at low concentration range in PEO−PVDF polymer-blend electrolyte (Figure 3a) probably results from the increased concentration of charge carriers. In the high salt concentration ("polymer-in-salt" conduction behavior region), the charged ionic clusters are expected to be formed.[44] These ionic clusters are considered to act as transient bridges and connect with each other to form segments of the infinite percolation pathways and exchange charges, which is the pathway for ion transportation in the "polymer-in-salt" conduction behavior region.[13] Florjanczyk et al.[45] believe that the changes in the ionic aggregates structure probably change the ionic conductive mechanism of the polymer matrix similar to that of conduction in glass. However, in the polymer-blend system studied, the DSC traces indicate that there is no presence of a crystalline phase of a complex formed by polymer and ionic agglomerates around T_m = 100 °C until a salt concentration of 37.9 wt % (EO:Li=2). The transition from "salt-in-polymer" to "polymer-in-salt" conduction behavior occurs at 23.4 wt % (EO:Li = 4). These indicate that the transition appears before an infinite percolation pathway is constructed by ionic clusters. This is consistent with the results that the "polymer-in-salt" conduction behavior is not totally dependent on the percolation pathway formed by ionic clusters and the polymer also takes an important role to influence this conduction behavior.[13,17] That is, in the case where clusters are not formed or connected, the polymer motion may play a significant part in determining the conductivity. Once the percolation pathway is formed, the conductivity is operated by percolation mechanism.

On the other hand, the transition from "salt-in-polymer" to "polymer-in-salt" conduction behavior occurs at the salt concentration of 23.4 wt %, which is much lower than 50 wt % as usually reported (Figure 3a). To further understand the contribution of PEO and PVDF to this lower shift in PEO−PVDF polymer-blend electrolyte, the conductivity of PEO−LiI and PVDF−LiI polymer electrolytes with various salt concentrations at 30 °C is studied, and the results are shown in Figure 3b. It is exhibited that both PEO and PVDF polymer electrolytes show the "polymer-in-salt" like conduction behavior above a salt concentration limit, which corresponds to 50.4 wt % for PEO electrolyte and 40.4 wt % for PVDF electrolyte, respectively. Compared to PEO system, PVDF polymer electrolytes show a higher conductivity with little changes as salt concentration increases. From the FTIR studies, Li^+ ions show strong association with PEO but not with PVDF (Table 1). As a result of this, the salt which is distributed into PVDF is more likely to form salt aggregations compared with that in PEO to support "polymer-in-salt" like conduction behavior as the salt concentration increases. So, we speculate that the lower shift of the transition in blend-based electrolytes may be largely attributed to the contribution of PVDF and the conduction behavior of PEO−PVDF polymer-blend electrolytes in the whole salt concentration studied is attributed to the effects of both PEO and PVDF in the electrolytes.

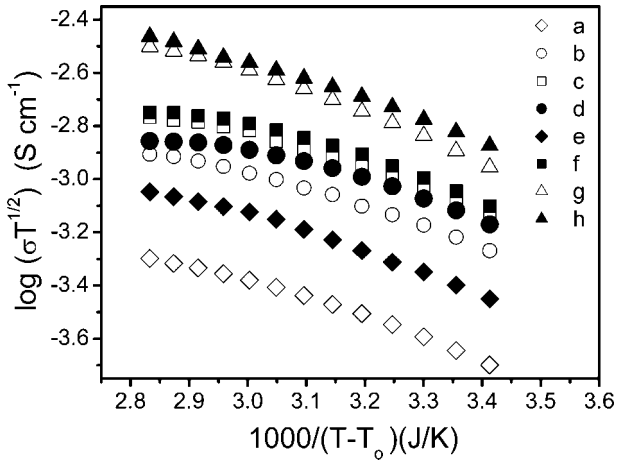

Figure 4. Temperature dependence of ionic conductivity of poly(ethylene oxide)−poly(vinylidene fluoride) polymer-blend electrolytes with different LiI concentrations (wt %): (a) 13.2%, (b) 14.8%, (c) 16.9%, (d) 19.6%, (e) 23.4%, (f) 28.9%, (g) 37.9%, and (h) 54.9%.

The temperature dependent ionic conductivity of the PEO−PVDF polymer-blend electrolytes with different LiI concentrations exhibits a typical Vogel−Tammann−Fulcher (VTF) conduction behavior (Figure 4), obeying the equation,[46]

$$\sigma(T) = AT^{1/2}\exp[(-B)/\kappa(T - T_0)] \quad (4)$$

where σ and T are the conductivity and absolute temperature values, respectively, κ is the Boltzmann constant, A is proportional to the number of the charge carriers, T_0 is regarded as 30−50K below the measured T_g ,[47] and B is the activation energy. Here, T_0 is defined as $T_0 = T_g - 50$ (K) and T_g as the glass transition temperature of the pure PEO−PVDF polymer blend.[32]

Li^+ Transference Numbers of PEO−PVDF Polymer-Blend Electrolytes with Different Salt Concentrations. For further understanding the transport properties of the PEO−PVDF polymer blend electrolytes, it is important to reveal the Li^+ transference numbers (t_+) in these composite electrolytes. Figure 5 shows the current relaxation curves during potentiostatic polarization at 25 °C for a polymer-blend electrolyte with salt concentrations of 13.2, 28.9, and 54.9 wt %. The insert is the initial complex impedance spectrum for the polymer blend electrolyte with the salt concentration of 54.9 wt %. From these curves, Li^+ transference number (t_+) was calculated according to eq 2 for the polymer electrolytes, and the data are presented in Table 2. It can be seen that the lithium transference numbers are decreasing from 0.39 to 0.22 as the salt concentration increases from 13.2 to 54.9 wt %. This may be explained by the cross-linking of the polymer chains with Li^+, and then by

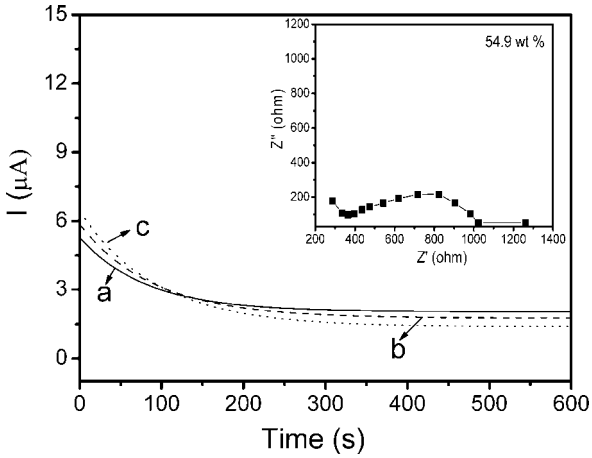

Figure 5. Current relaxation curves during potentiostatic polarization (cell area = 1.76 cm^{-2}, T = 25 °C, V = 500 mV) for PEO−PVDF polymer blend electrolytes with various salt concentrations (wt %): (a) 13.2% (solid line) (b) 23.4% (dashed line), and (c) 54.9% (dotted line). The inset is the initial complex impedance diagram for PEO−PVDF polymer blend electrolyte with 54.9 wt % LiI concentration.

TABLE 2: Transference Numbers of PEO−PVDF Polymer-Blend Electrolytes with Different Salt Concentrations at 25 °C

LiI concentrations (wt %)	Li^+ transference numbers (t_+)
13.2	0.39
23.4	0.29
54.9	0.22

the increased salt aggregates as the salt concentration increases, with consequent decrease in cation migration. The low Li^+ transference numbers ($t_+ = 0.39-0.22$) indicates that the ionic conductivity of the PEO−PVDF polymer blend electrolyte is dominated by anionic (I^-) motion. These results are close to the Li^+ transference number studies on PEO−LiI system ($t_+ = 0.31$) determined by Strauss et al,[21] and a low lithium transference number is expected to be advantageous for the performances of the corresponding DSSC with this polymer-blend electrolyte.

Most of "polymer-in-salt" electrolytes reported are based on PAN or its copolymers, which are expected to provide high cationic transport number, and most of the studies attribute this "polymer-in-salt" conduction behavior to the formation of continuous connected positive ionic cluster. Due to the decoupled nature of the PAN with the lithium salt, the PAN based electrolytes undoubtedly can provide much high lithium transport than the PEO based system, which has a strong interaction with the lithium salt. However, some recent studies indicate that whether or not the cation is the dominant charge carrier in the "polymer-in-salt" electrolyte is not clearly known and, indeed, the nature of the polymer may have some influence over this.[48] Just as we mentioned above, both the polymer and the ionic cluster will influence the "polymer-in-salt" conduction behavior. Whether or not the cation is the dominant charge carrier depends on the nature of the polymer matrix.

Salt Effect on the Surface Morphology of PEO−PVDF Polymer-Blend Electrolytes. Figure 6 shows scanning electron microscopy of four polymer-blend electrolyte membranes with different salt concentration (0, 13.2, 28.9, and 54.9 wt %). The pure PEO−PVDF polymer blend (Figure 6a) displays a surface with rough spherulites and pores owing to the crystallization of the polymer matrix. However, as the salt increases to 13.2 wt % (Figure 6b), the surface of the spherulites becomes smooth and some amorphous regions between spherulites are observed, showing a reduction of the crystallization due to the dissolving of the salt. With higher salt concentration at 28.9 wt % (Figure 6c), a comparatively compact and smooth surface is observed, in which the porosity and the spherulite have disappeared. The disappearance of the porosity and the grain is considered to be advantageous for interfacial contact between the nanocrystalline TiO_2 electrode and the polymer electrolyte. When the salt increases to 54.9 wt % (Figure 6d), severe salt aggregates are observed. Some of these aggregates are dispersed and some of them connect with each other to form partially continuous pathway. They both take important roles for the ionic transport in "polymer-in-salt" electrolytes as well as the polymer.[49]

Current−Voltage Characteristics of PEO−PVDF Polymer-Blend Electrolytes with Different Salt Concentration. Photocurrent density/voltage characteristics of N3-sensitized nanocrystalline TiO_2 film solar cells using PEO−PVDF polymer-blend electrolytes with various LiI concentrations (13.2−54.9 wt %) and $LiI/I_2 = 10$ (molar ratio) were measured under an illumination intensity of 53.6 mW cm^{-2} (AM 1.5), and the results are presented in Figure 7. The dependence of J_{sc}, V_{oc}, the fill factor (FF), and the photo-to-current conversion efficiency (η) on the LiI concentration is shown in Figure 8. It is observed that the J_{sc} increases from 2.76 to 5.76 mA cm^{-2} when the LiI concentration increases from13.2 to 28.9 wt %. Further increasing of the LiI concentration leads to a decrease of J_{sc}. When the salt concentration increases to 54.9 wt %, J_{sc} decreases to 3.4 mA cm^{-2} (Figure 8d). V_{oc} and FF increase gradually with increasing LiI concentration (Figure 8b, c). The poor FF (<0.5) at low LiI concentration is consistent with the depletion of the I_3^- concentration at the Pt cathode.[50] Furthermore, because of low conductivity of the electrolytes with low LiI content, the FF of this electrolyte is poor due to the higher series resistance of the cells compared to that of higher salt concentration ones.[51] A maximum efficiency of 3.26% (Figure 8a) is obtained from the DSSC fabricated with LiI concentration of 28.9 wt % (EO: Li = 3).

It is known that an efficient transport of iodide and triiodide in the electrolyte is necessary for good performance of the DSSC:

$$I^- + I_2 \leftrightarrows I_3^- + I_2 \leftrightarrows I_5^- \quad (5)$$

$$3I^- + 2dye^+ \rightarrow I_3^- + 2dye\ (TiO_2\ photoanode) \quad (6)$$

$$I_3^- + 2e^- \leftrightarrows 3I^-\ (counter\ electrode) \quad (7)$$

The dark reaction occurring will deteriorate the performance of the DSSC:

$$I_3^- + 2e^-(TiO_2CB) \rightarrow 3I^- \quad (8)$$

To investigate the effects of I^- and I_3^- concentration on the performances of DSSC with PEO−PVDF polymer-blend electrolytes of different LiI concentration, the UV−vis absorptions of these electrolytes are measured (Figure 9). As is seen, the peaks around 290 and 360 nm indicate the presence of I_3^-[52] and the peak around 226 nm is that of I^-.[53] The intensity and width of the absorption peaks at 229, 291, and 362 nm in the spectrum increase with salt concentration, implying an increase of both I^- and I_3^- concentration in the electrolytes. When LiI concentration reaches 54.9 wt %, the light absorption extends to 450 nm in this electrolyte solution

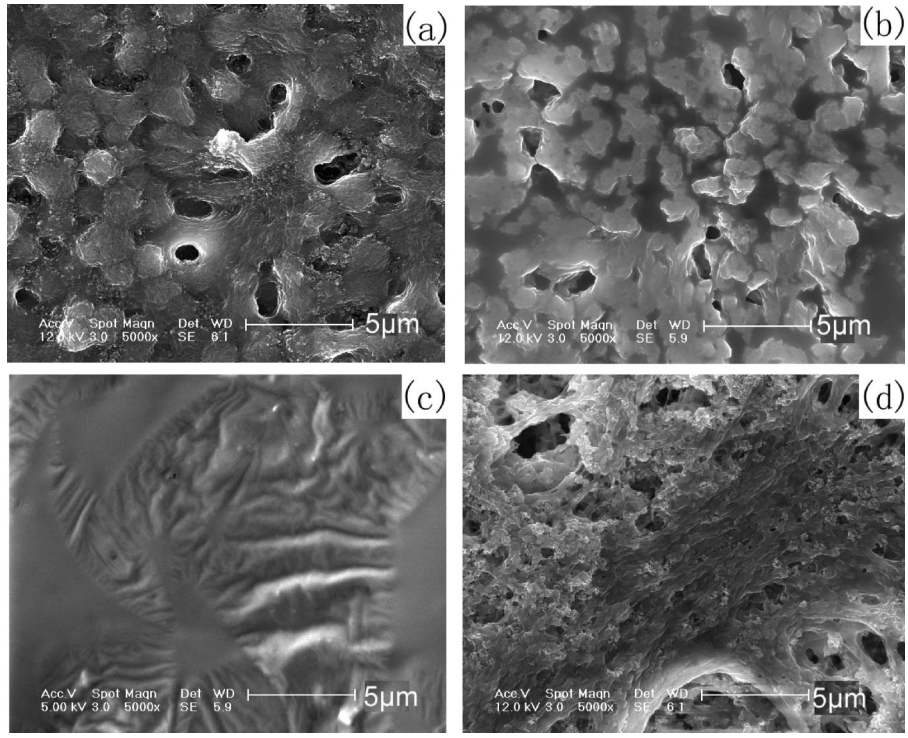

Figure 6. SEM images of the polymer-blend electrolytes based on poly(ethylene oxide)−poly(vinylidene fluoride) with different LiI concentrations (wt %): (a) 0, (b) 13.2, (c) 28.9, and (d) 54.9%.

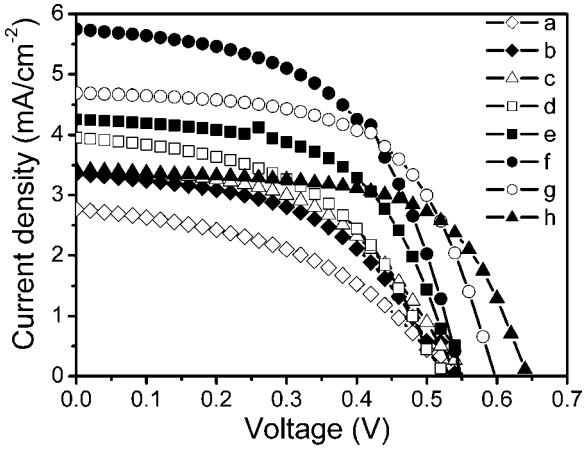

Figure 7. Photcurrent−voltage curve of the DSSC with poly(ethylene oxide)−poly(vinylidene fluoride) polymer-blend electrolytes with various LiI concentrations (wt %): (a) 13.2, (b) 14.8, (c) 16.9, (d) 19.6, (e) 23.4, (f) 28.9, (g) 37.9, and (h) 54.9%.

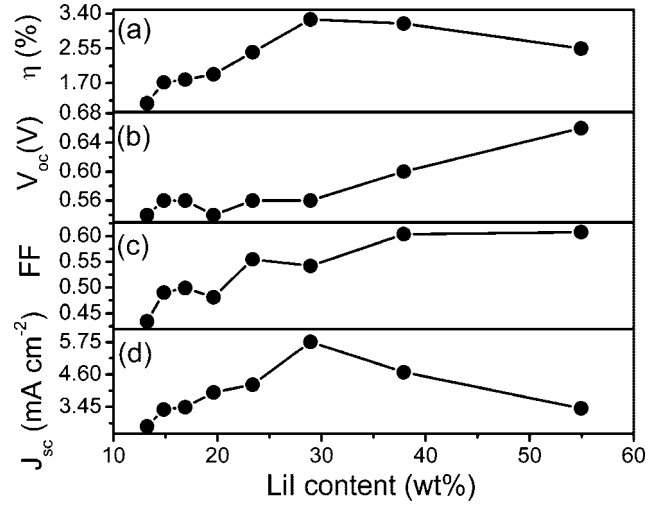

Figure 8. Variation of (a) photo-to-current conversion efficiency η, (b) open-circuit voltage V_{oc}, (c) fill factor (FF), and (d) short-circuit photocurrent density J_{sc} with LiI concentraion in the poly(ethylene oxide)−poly(vinylidene fluoride) polymer-blend electrolytes.

(Figure 9h). The increased absorption in visible light by I_3^- does not contribute to the net output current of DSSC but weakens the light absorption of dye, which makes the J_{sc} value to decrease. As is seen in Figure 8d, J_{sc} is mainly affected by the slow diffusion of I_3^- at low LiI concentrations ($\leq$28.9 wt %).[54] So, an increase of I_3^- concentration leads to an increase of J_{sc}. At high LiI concentrations (>28.9 wt %), the decrease of J_{sc} is mainly due to the increased charge recombination at the photoanode/electrolyte interface with enhanced concentration of I_3^- beyond a limitation.[55]

For the DSSC based on the PEO−PVDF polymer-blend electrolytes, the V_{oc} increases significantly from 0.54 to 0.66 V as the concentration of LiI increases from 13.2 to 54.9 wt %, corresponding to a voltage shift of 120 mV (Figure 8b). A similar phenomenon in lithium battery has been reported in PEO$_n$LiTFSI system.[56] It is speculated that the increasing of V_{oc} with salt content originates in the plasticizing effect of the salt in PEO$_n$LiTFSI electrolyte.[57] As for the photoelectrochemical system studied, this can be understood by the theoretical considerations:[50]

$$n = n_0 \exp(qV/kT) \tag{9}$$

where n and n_0 represent the electron population in the semiconductor present in the light and in the dark, respectively, k is the Boltzmann constant, T is the absolute temperature, q is the electronic charge, and V is the photovoltage. $qV = E_f - E_{fo}$; E_f and E_{fo} are the respective Fermi levels of TiO_2 in the

light and in the dark.

and

$$V_{oc} = \frac{kT}{q}\left(\ln\frac{AI_0}{n_0 k_{et} c_{ox}}\right) \quad (10)$$

where A is the ratio of absorbed photo flux to I_0, k_{et} is the rate constant for back electron transfer, and c_{ox} is the concentration of the oxidized half of the redox couple ($[I_3^-]$).

Because the redox potential of I^-/I_3^- was held constant by maintaining the concentration ratio of LiI/I_2, a larger electron concentration in TiO_2 implies a higher V_{oc} (eq 9). With an increase of the initial I^- ions as the salt concentration increases in the electrolytes (Figure 9), the regeneration of the oxidized dye is expected to be accelerated (eq 6) and the accumulated electrons in TiO_2 via charge injection from excited dye molecules increase, resulting in a higher V_{oc}. On the other hand, from an examination of eq 10, the photovoltage of a DSSC is limited by the dark reaction occurring in the photoelectrochemical system (eq 8), where the electrons from the conduction band of TiO_2 recombine with the oxidized species (I_3^-) of the redox couple. Increasing the LiI content leads to enhanced concentration of I_3^- (Figure 9), and an increased charge recombination occurs when I_3^- concentration exceeds a critical point, resulting in a decreased V_{oc}. Therefore, we suppose that these two compensated effects mentioned above compete with each other as the salt content increases and result in the final increasing of the V_{oc}, as seen in Figure 8b.

Besides, it should be pointed out that the free lithium ions can easily penetrate into TiO_2 surface or even lattice, changing the electron concentration in TiO_2.[19,58] Thus, if the concentration of free lithium ions in the electrolytes increases as the LiI concentration increases, it will affect both the photocurrent and the photovoltage of the DSSC. However, in the PEO−PVDF polymer-blend electrolytes studied here, the Li^+ transference numbers are very low ($t_+ = 0.39-0.22$) and the Li^+ ions have shown strong interactions with the polymer matrix as the salt concentration increases and form salt aggregates at the high salt concentrations, as exhibited in DSC and SEM studies. Therefore, it is reasonable to postulate that the free Li^+ ions contribute less to the performances of DSSC compared with I^- and I_3^- ions.

Taking into consideration the dependence of conductivity, surface morphology characteristics, FF, J_{sc}, and V_{oc} on the LiI content, as discussed above, an optimized conversion efficiency of 3.26% is achieved for DSSC with PEO−PVDF polymer-blend electrolyte at the LiI concentration of 28.9 wt %, due to its high conductivity, improved interfacial contact, maximum photocurrent, and relatively high photovoltage.

Conclusions

A "polymer-in-salt" like conduction behavior was reported in the electrolyte based on lithium iodide and PEO−PVDF polymer blend. Through DSC, FTIR, SEM, impedance spectra, Li^+ transference number measurement, and UV−vis investigations, we studied the conduction behavior of the polymer-blend electrolytes in the high salt concentration and the salt effect on the performances of corresponding DSSC in detail. The introduction of high salt concentrations (>23.4 wt %) results in highly conducting electrolyte systems, similar in characteristic to that of "polymer-in-salt" electrolytes. FTIR investigations show a strong interaction between ions and polymer matrix. The ionic aggregates are not observed until the salt concentration reaches 37.9 wt % from DSC and SEM characterization. Because the transition from "salt-in-polymer" to "polymer-in-salt" conduction behavior at the salt concentration of 23.4 wt % appears before an infinite percolation pathway is formed, we suggest that both ion aggregates and the polymer matrix contribute to the "polymer-in-salt" conduction behavior in PEO−PVDF polymer-blend electrolytes. The cationic transference number (t_+) results ($t_+ = 0.39-0.22$) reveal that the ionic conductivity of the PEO−PVDF polymer blend electrolyte is dominated by anionic (I^-) motion and the t_+ decreases as the salt concentration increasing. The short-circuit photocurrent density (J_{sc}) of the corresponding DSSC initially increases and then decreases with increasing LiI content. At low LiI concentrations (≤28.9 wt %), the J_{sc} is mainly affected by the mobility of I_3^-. At high LiI concentrations (>28.9 wt %), the decreased J_{sc} results from the increased charge recombination. The V_{oc} increases with the salt content due to the increased I^- concentration and to the larger electron concentration in TiO_2. A 3.26% of photo-to-current conversion efficiency based on the PEO−PVDF polymer-blend electrolytes is obtained at the optimum LiI concentration of 28.9 wt % in "polymer-in-salt" region with high ionic conductivity (1.06×10^{-3} S cm^{-1}) under the radiation of 53.6 mW cm^{-2} (AM 1.5).

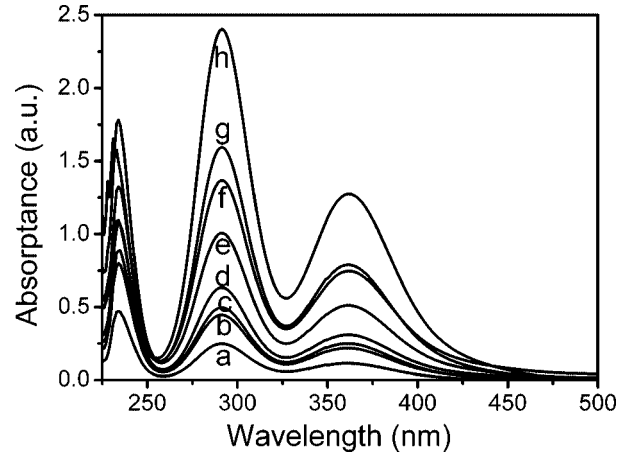

Figure 9. UV−vis spactra of poly(ethylene oxide)−poly(vinylidene fluoride) polymer-blend electrolytes varying with LiI concentrations (wt %): (a) 13.2, (b) 14.8, (c) 16.9, (d) 19.6, (e) 23.4, (f) 28.9, (g) 37.9, and (h) 54.9%.

Acknowledgment. We acknowledge the financial support of the Ministry of Science and Technology of China through Hi-Tech plan (funding No. 2006AA03Z347) and the partial financial support from the National Nature Science Foundation of China (50125309). We also acknowledge the help of the Nanoscience and Nanotechnology Centre at Wuhan University for the DSC measurements.

References and Notes

(1) O'Regan, B.; Grätzel, M. *Nature* **1991**, *353*, 737.
(2) Grätzel, M. *Inorg. Chem.* **2005**, *44*, 6841.
(3) Meng, Q. B.; Takahashi, K.; Zhang, X. T.; Sutanto, I.; Rao, T. N.; Sato, O.; Fujishima, A. *Langmuir* **2003**, *19*, 3572.
(4) Hirata, N.; Kroeze, J. E.; Park, T.; Jones, D.; Haque, S. A.; Holmes, A. B.; Durrant, J. R. *Chem. Commun.* **2006**, 535.
(5) Wang, P.; Zakeeruddin, S. M.; Moser, J-E.; Grätzel, M. *J. Phys. Chem. B* **2003**, *107*, 13280.
(6) Wang, P.; Zakeeruddin, S. M.; Moser, J-E.; Nazeeruddin, M. K.; Sekiguchi, T.; Grätzel, M. *Nat. Mater.* **2003**, *2*, 402.
(7) Stergiopoulos, T.; Arabatzis, I. M.; Katsaros, G.; Falaras, P. *Nano Lett.* **2002**, *2*, 1259.
(8) Wu, J. H.; Lan, Z.; Wang, D. B.; Hao, S. C.; Lin, J. M.; Huang, Y. F.; Yin; S.; SatoT., *Electrochim. Acta* **2006**, *51*, 4243.
(9) Li, M. Y.; Feng, S. J.; Fang, S. B.; Xiao, X. R.; Li, X. P.; Zhou, X. W.; Lin, Y. *Electrochim. Acta* **2007**, *52*, 4858.

(10) Kang, M-S.; Kim, J. H.; Kim, Y. J.; Won, J.; Park, N-G.; Kang, Y. S. *Chem. Commun.* **2005**, 88.
(11) Wu, J. H.; Li, P. J.; Hao, S. C.; Yang, H. X.; Lan, Z. *Electrochim. Acta* **2007**, *52*, 5334.
(12) Angell, C. A.; Liu, C.; Sanchez, E. *Nature* **1993**, *362*, 137.
(13) Ferry, A.; Edman, L.; Forsyth, M.; MacFarlane, D. R.; Sun, J. *J. Appl. Phys.* **1999**, *86*, 2346.
(14) Forsyth, M.; Sun, J.; MacFarlane, D. R. *Solid State Ionics* **1998**, *112*, 161.
(15) Forsyth, M.; Sun, J.; MacFarlane, D. R.; Hill, A. J. *J. Polym. Sci., B: Polym. Phys.* **2000**, *38*, 341.
(16) Wang, Z.; Gao, W.; Chen, L.; Mo, Y.; Huang, X. *Solid State Ionics* **2002**, *51*, 154.
(17) Bushkova, O. V.; Zhukovsky, V. M.; Lirova, B. I.; Kruglyashov, A. L. *Solid State Ionics* **1999**, *119*, 217.
(18) Forsyth, M.; MacFarlane, D. R.; Hill, A. J. *Electrochim. Acta* **2000**, *45*, 1243.
(19) Kuang, D. B.; Klein, C.; Snaith, H. J.; Moser, J-E.; Humphry-Baker, R.; Comte, P.; Zakeeruddin, S. M.; Grätzel, M. *Nano lett.* **2006**, *4*, 769.
(20) Alloin, F.; Benrabah, D.; Sanchez, J.-Y. *J. Power Sources* **1997**, *68*, 372.
(21) Strauss, E.; Golodnitsky, D.; Ardel, G.; Peled, E. *Electrochim. Acta* **1998**, *43*, 1315.
(22) Stergiopoulos, T.; Araatzis, I. M.; Katsaros, G.; Falaras, P. *Nano Lett.* **2002**, *2*, 1259.
(23) Kim, J. H.; Kang, M. S.; Kim, Y. J.; Won, J.; Park, N. G.; Kang, Y. S. *Chem. Commun.* **2004**, 1662.
(24) Bruce, P. G.; Vincent, C. A. *J. Chem. Soc., Faraday Trans.* **1993**, *89*, 3187.
(25) Ferry, A. *J. Phys. Chem. B* **1997**, *101*, 150.
(26) Jacob, M. M. E.; Prabaharan, S. R. S.; Radhakrishna, S. *Solid State Ionics* **1997**, *104*, 267.
(27) Han, H. W.; Liu, W.; Zhang, J.; Zhao, X. Z. *Adv. Funct. Mater.* **2005**, *15*, 1940.
(28) Zhang, J.; Han, H. W.; Wu, S. J.; Xu, S.; Zhou, C. H.; Yang, Y.; Zhao, X. Z. *Nanotechnology* **2007**, *18*, 295606.
(29) Wang, H. X.; Wang, Z. X.; Xue, B. F.; Meng, Q. B.; Huang, X. J.; Chen, L. Q. *Chem. Commun.* **2004**, 2186.
(30) Wang, H. X.; Li, H.; Xue, B. F.; Wang, Z. X.; Meng, Q. B.; Chen, L. Q. *J. Am. Chem. Soc.* **2005**, *127*, 6394.
(31) Evans, J.; Vincent, C. A.; Bruce, P. G. *Polymer* **1987**, *28*, 2324.
(32) Croce, F.; Curini, R.; Pantaloni, S.; Selvaggi, A.; Scrosati, B. *J. Appl. Electrochem.* **1988**, *18*, 401.
(33) Watanabe, M.; Nagano, S.; Sanui, K.; Ogata, N. *Solid State Ionics* **1998**, *28*−*30*, 911.
(34) Reiche, A.; Tübke, J.; Sandner, R.; Werther, A.; Sandner, B.; Fleischer, G. *Electrochim. Acta* **1998**, *43*, 1429.
(35) Dai, Y.; Wang, Y.; Greenbaum, S. G.; Bajue, S. A.; Golodnitsky, D.; Ardel, G.; Strauss, E.; Peled, E. *Electrochim. Acta* **1998**, *43*, 1557.
(36) Angell, C. A.; Fan, J.; Liu, C.; Lu, Q.; Sanchez, E.; Xu, K. *Solid State Ionics* **1994**, *69*, 343.
(37) Perrier, M.; Besner, S.; Paquette, C.; Valee, A.; Prud'homme, J. *Electrochim. Acta* **1995**, *40*, 2123.
(38) Ferry, A.; Jacobson, P.; Torrel, L. M. *Electrochim. Acta* **1995**, *40*, 2369.
(39) Wieczorek, W.; Lipka, P.; Zukowska, G.; Wycislik, H. *J. Phys. Chem. B* **1998**, *102*, 6968.
(40) Bernson, A.; Lindgren, J.; Huang, W. W.; Frecn, R. *Polymer* **1995**, *36*, 4471.
(41) Zhu, H.; Ma, Y. G.; Fan, Y. G.; Shen, J. C. *Thin Solid Films* **2001**, *397*, 95.
(42) Parida, S. K.; Dash, S.; Patel, S.; Mishra, B. K. *Adv. Colloid Interface Sci.* **2006**, *121*, 77.
(43) Wang, Z. X.; Gao, W. D.; Chen, L. Q.; Mo, Y. J.; Huang, X. J. *Solid State Ionics* **2002**, *154*−*155*, 51.
(44) Stygar, J.; Biernat, A.; Kwiatkowska, A.; Lewandowski, P.; Rusiecka, A.; Zalewska, A.; Wieczorek, W. *J. Phys. Chem. B* **2004**, *108*, 4263.
(45) Florjanczyk, Z.; Zygadło-Monikowska, E.; Wieczorek, W.; Ryszawy, A.; Tomaszewska, A.; Fredman, K.; Golodnitsky, D.; Peled, E.; Scrosati, B. *J. Phys. Chem. B* **2004**, *108*, 14907.
(46) Gnanaraj, J. S.; Karekar, R. N.; Skaria, S.; Rajan, C. R.; Ponrathnam, S. *Polymer* **1997**, *38*, 3709.
(47) Siekierski, M.; Wieczorek, W.; Przyłuski, J. *Electrochim. Acta* **1998**, *43*, 1339.
(48) Forsyth, M.; Sun, J. Z.; MacFarlane, D. R. *Electrochim. Acta* **2000**, *45*, 1249.
(49) Wang, H. X.; Wang, Z. X.; Li, H.; Meng, Q. B.; Chen, L. Q. *Electrochim. Acta* **2007**, *52*, 2039.
(50) Huang, S. Y.; Schlichthorl, G.; Nozik, A. J.; Grätzel, M.; Frank, A. J. *J. Phys. Chem. B* **1997**, *101*, 2576.
(51) Ngamsinlapasathian, S.; Sakulkhaemaruethai, S.; Pavasupree, S.; Kitiyanan, A.; Sreethawong, T.; Suzuki, Y.; Yoshikawa, S. *J. Photochem. Photobiol., A* **2004**, *164*, 145.
(52) Kebede, Z.; Lindquist, S-E. *Sol. Energy Mater. Sol. Cells* **1999**, *57*, 259.
(53) Allsopp, C. B. *Proc. R. Soc. London, Ser. A* **1937**, paper 167.
(54) Wang, H. X.; Liu, X. Z.; Wang, Z. X.; Li, H.; Li, D. M.; Meng, Q. B.; Chen, L. Q. *J. Phys. Chem. B* **2006**, *110*, 5970.
(55) Papageorgiou, N.; Athanassov, Y.; Kitamura, T.; Armand, M.; Bonhote, P.; Pettersson, H.; Azam, A.; Grätzel, M. *J. Electrochem. Soc.* **1996**, *143*, 3099.
(56) Edman, L.; Doeff, M. M.; Ferry, A.; Kerr, J.; De Jonghe, L. C. *J. Phys. Chem. B* **2000**, *104*, 3476.
(57) Sung, J. P.; Young, C. B. *J. Appl. Electrochem.* **2005**, *35*, 259.
(58) Nakade, S.; Kanzaki, T.; Kubo, W.; Kitamura, T.; Wada, Y.; Yanagida, S. *J. Phys. Chem. B* **2005**, *109*, 3480.

JP801156H